Interaction and Multiscale Mechanics, Vol. 5, No. 3 (2012) 169-185
DOI: http://dx.doi.org/10.12989/imm.2012.5.3.169

Time-frequency analysis of a coupled bridge-vehicle system with breathing cracks

W.J. Wang, Z.R. Lu* and J.K. Liu

Department of Applied Mechanics, Sun Yat-sen University, Guangzhou, Guangdong Province, 510006, P.R. China

(Received March 22, 2012, Revised April 20, 2012, Accepted May 14, 2012)

Abstract. The concrete bridge is likely to produce fatigue cracks during long period of service due to the moving vehicular loads and the degeneration of materials. This paper deals with the time-frequency analysis of a coupled bridge-vehicle system. The bridge is modeled as an Euler beam with breathing cracks. The vehicle is represented by a two-axle vehicle model. The equation of motion of the coupled bridge-vehicle system is established using the finite element method, and the Newmark direct integration method is adopted to calculate the dynamic responses of the system. The effect of breathing cracks on the dynamic responses of the bridge is investigated. The time-frequency characteristics of the responses are analyzed using both the Hilbert-Huang transform and wavelet transform. The results of time-frequency analysis indicate that complicated non-linear and non-stationary features will appear due to the breathing effect of the cracks.

Keywords: bridge-vehicle system; dynamic response; time-frequency analysis; Hilbert-Huang transform; wavelet transform.

1. Introduction

The dynamic responses of bridges subjected to moving vehicles have been studied in the past few decades (Yener and Chompooming 1994, Kou and Dewolf 1997, Pan and Li 2002). The dynamic responses of coupled vehicle/train-bridge systems have been studied extensively in recent years (Yang and Yau 1997, Zhang *et al*. 2005, Sun and Luo 2007, Yau 2009, Yang *et al*. 2010, Li and Zhu 2010). Some scholars also studied the effect of road roughness on the dynamic responses of the coupled vehicle-bridge system (Law and Zhu 2004, Chang *et al*. 2010). Cojocaru and Irschik (2010) studied the dynamic response of an elastic bridge loaded by a moving elastic beam with a finite length. Wang *et al*. (2010) investigated the nonlinear dynamic responses of a long-span bridge using a complex wind-train-bridge system model.

The concrete bridges are likely to produce fatigue cracks due to the moving vehicles and the degeneration of materials. The flexural rigidity of the bridge will be reduced due to these cracks, which may greatly affect the dynamic responses of the bridge. The dynamic responses of a cracked

* Corresponding author, Professor, E-mail: lvzhr@mail.sysu.edu.cn

bridge has been investigated by many researchers. Mahmoud (2001) studied the effect of cracks on the dynamic responses of a simple beam subjected to a moving load. Mahmoud and Abou Zaid (2002), Ariaei *et al*. (2009) discussed the dynamic responses of a beam with a crack subjected to moving masses. Law and Zhu (2005) investigated the dynamic behavior of a damaged concrete simply supported bridge under moving vehicular loads.

Generally, there are two kinds of crack model in the existing literature: open crack model (Abdel *et al*. 1999, Binici 2005, Aydin 2008, Lu and Law 2009) and breathing crack model (Chondros *et al*. 2001, Law and Zhu 2004, Douka and Hadjileontiadis 2005, Mahmoud 2001, Ariaei *et al*. 2009). Most researchers assume the cracks to remain open during the vibration of the structure. On the other hand, a breathing crack will open and close with time depending on the load conditions and vibration amplitudes. In fact, different crack models may lead to different conclusions. There are a lot of researches in the literature regarding the vibration analysis of structures containing open cracks (Aydin 2008, Lu and Law 2009). There are also many researches dealing with the bridge-vehicle system with multiple breathing cracks (Mahmoud 2001, Ariaei *et al*. 2009).

There exist several signal processing tools to analyze the response characteristics of structures, such as the fast Fourier transform (FFT), wavelet transform (WT) and Hilbert-Huang transform (HHT). Law and Zhu (2005) investigated the nonlinear characteristics of the reinforced concrete structures under vehicular loads using the FFT transform. It is known that WT and HHT are especially useful for the analysis of non-stationary data. Some scholars analyzed the non-stationary characteristics of wind effects on tall buildings with HHT (Li and Wu 2007, Chen *et al*. 2011). Kim and Melhem (2003) conducted damage detection in a simply supported pre-stressed beam with both FFT and continuous wavelet transform. Zhu and Law (2007) discussed the nonlinear characteristics in the vibration response of a reinforced concrete beam with cracks using the Hilbert-Huang spectrum. An *et al*. (2010) established a simply-supported cracked beam subjected to a moving spring-mass system and studied the damage detection using the wavelet analysis. Chakraborty and Basu (2008) developed an input-output relation for the non-stationary responses of long-span bridges subjected to random differential support motions with continuous wavelet transform.

This paper aims to investigate the time-frequency analysis of a coupled bridge-vehicle system with breathing cracks. The vehicle is represented as a two-axle vehicle model, and the bridge is modeled as a continuous damaged Euler-Bernoulli beam with breathing cracks. The equation of motion for the coupled vehicle-bridge system is established using the finite element method, and the Newmark direct integration method is used to calculate the dynamic responses of the system. The effects of different numbers and the positions of the cracks on the vibration responses of the bridge are studied. The roughness of the bridge is also taken into account. The time-frequency feature of the dynamic response is analyzed using both the HHT and WT. The results from time-frequency analysis indicate that complicated non-linear or non-stationary feature will appear due to the breathing effect of the cracks.

2. Theory and formulation

2.1 Vehicle-bridge system

Fig. 1 shows a vehicle-bridge system under study. The equations of motion for the vehicle and the bridge are obtained as follows.

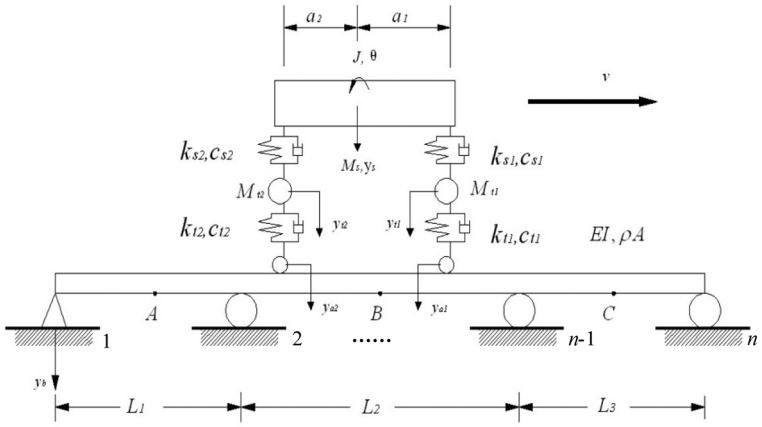

Fig. 1 Vehicle-bridge system under study

2.1.1 Equation of motion of the vehicle

According to the d'Alembert principle, the equation of motion for the vehicle is expressed as

$$[M_v]\{\ddot{y}_v\} + [C_v]\{\dot{y}_v\} + [K_v]\{y_v\} = \{F_v\} \tag{1}$$

where $\{y_v\} = \{y_s, \theta, y_{t1}, y_{t2}\}^T$ is the response vector, $\{F_v\} = \{0, 0, k_{t1}y_{a1} + c_{t1}\dot{y}_{a1}, k_{t2}y_{a2} + c_{t2}\dot{y}_{a2}\}^T$ is the excitation force vector, and $[M_v], [C_v], [K_v]$ are the mass, damping and stiffness matrices of the vehicle, respectively. The detailed expressions for these matrices are written as

$$M_v = \begin{bmatrix} M_s & & & \\ & J & & \\ & & M_{t1} & \\ & & & M_{t2} \end{bmatrix}, \quad C_v = \begin{bmatrix} c_{s1}+c_{s2} & c_{s1}a_1 - c_{s2}a_2 & -c_{s1} & -c_{s2} \\ c_{s1}a_1 - c_{s2}a_2 & c_{s1}a_1^2 + c_{s2}a_2^2 & -c_{s1}a_1 & c_{s2}a_2 \\ -c_{s1} & -c_{s1}a_1 & c_{s1}+c_{t1} & 0 \\ -c_{s2} & c_{s2}a_2 & 0 & c_{s2}+c_{t2} \end{bmatrix}$$

$$K_v = \begin{bmatrix} k_{s1}+k_{s2} & k_{s1}a_1 - k_{s2}a_2 & -k_{s1} & -k_{s2} \\ k_{s1}a_1 - k_{s2}a_2 & k_{s1}a_1^2 + k_{s2}a_2^2 & -k_{s1}a_1 & k_{s2}a_2 \\ -k_{s1} & -k_{s1}a_1 & k_{s1}+k_{t1} & 0 \\ -k_{s2} & k_{s2}a_2 & 0 & k_{s2}+k_{t2} \end{bmatrix}$$

2.1.2 Equation of motion of the bridge

After finite element discretization, the forced vibration equation for the bridge can be written as

$$[M_b]\{\ddot{y}_b\} + [C_b]\{\dot{y}_b\} + [K_b]\{y_b\} = \{F_b\} \tag{2}$$

where $\{y_b\}$ is the vertical displacement, $\{F_b\}$ is the nodal force vector, and $[M_b], [C_b], [K_b]$ are the system mass, damping and stiffness matrices of the bridge. In this paper the Rayleigh damping model is adopted, i.e., $[C_b] = a_1[M_b] + a_2[K_b]$, where a_1 and a_2 are two constants.

2.1.3 Equation of motion of the vehicle-bridge system

The vehicle-bridge system is treated as two dynamic sub-systems in this paper, i.e., the vehicle and the bridge. The interaction forces between the vehicle and the bridge are regarded as the external forces for each sub-system. We assume that there is a close contact between the wheel and the bridge deck all the time. The equation of motion of the coupled vehicle-bridge system is expressed as

$$\left.\begin{aligned}[M_b]\{\ddot{y}_b\}+[C_b]\{\dot{y}_b\}+[K_b]\{y_b\} &= \{F_b\}\\ [M_v]\{\ddot{y}_v\}+[C_v]\{\dot{y}_v\}+[K_v]\{y_v\} &= \{F_v\}\end{aligned}\right\} \tag{3}$$

The interaction force between the bridge and the vehicle can be written as

$$\begin{cases}P_1 = (M_{t1}+M_s a_2)g+k_{t1}(y_{t1}-y_{a1})+c_{t1}(\dot{y}_{t1}-\dot{y}_{a1})\\ P_2 = (M_{t2}+M_s a_1)g+k_{t2}(y_{t2}-y_{a2})+c_{t2}(\dot{y}_{t2}-\dot{y}_{a2})\end{cases} \tag{4}$$

where y_{ai} (i=1, 2) is the vertical displacement of the contact point between the ith wheel and the bridge, which can be expressed as

$$y_{ai} = y_b(x_i(t), t)+r_i(x_i(t)) \tag{5}$$

Here r_i is the road roughness. If the road roughness is zero, $y_{ai} = y_b(x_i(t), t)$.

The nodal force vector $\{F_b\}$ in Eq. (3) can be obtained using the shape function matrix $[N]$ of the beam element

$$\{F_b\} = \sum_{i=1}^{2}[N]\{P_i\} \tag{6}$$

Differentiating with respect to time on both sides of Eq. (5), one has

$$\dot{y}_{ai} = \frac{\partial y_b}{\partial x_i}\frac{\partial x_i}{\partial t}+\frac{\partial y_b}{\partial t}+\frac{\partial r}{\partial x_i}\frac{\partial x_i}{\partial t} \tag{7}$$

The Newmark direct integration method is used to obtain the dynamic responses of the bridge-vehicle system as shown in Eq. (3).

2.2 Modeling of the crack in the bridge

2.2.1 Open crack model

Abdel Wahab *et al*. (1999) modeled the cracked beam as a reduction in the Young's modulus of the material. The evolution of damage along the beam length was described through an experimental work. Fig. 2 shows the distribution of the Young's modulus along the beam.

$$\left.\begin{aligned}E(x) &= E_0\left(1-(1-\alpha)\cos^2\left(\frac{\pi}{2}\left(\frac{x}{\beta L/2}\right)^n\right)\right), \text{for}(0<x<\beta L/2)\\ E &= E_0, \text{for}(\beta L/2\le x\le L/2)\end{aligned}\right\} \tag{8}$$

where L is the length of the beam, x is the distance along the beam measured from the center line,

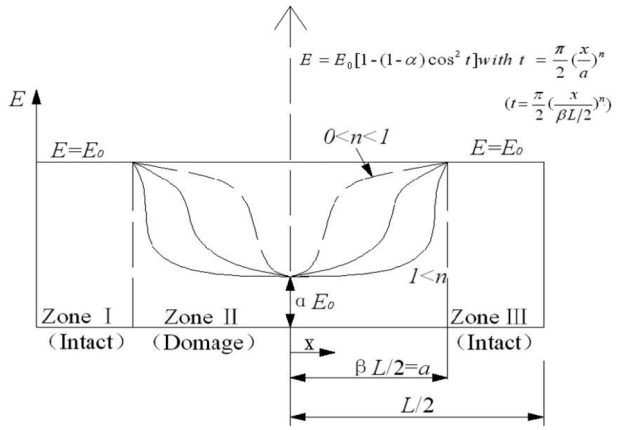

Fig. 2 Symmetric damage function by Abdel Wahab *et al*. (1999)

and α, β, n are the parameters of the crack damage. α characterizes the magnitude of the crack, which lies between 0 and 1. If α is equal to 1, no crack is presented, whereas if α drops to zero, the bending stiffness will vanish at the middle-point of the beam. β characterizes the length of the crack zone, and it lies between 0 and 1. Parameter n characterizes the variation of the E-modulus from the center of the beam to the end of the crack zone. E_0 is the modulus of the intact beam.

2.2.2 Breathing crack model

Actually, during the operation stages of the bridge, the depth of the crack will vary with the moving vehicle instead of open all the time. The crack opening/closing behavior can be simulated by elastic-stiffness recovery during the elastic unloading process from tensile state to compressive state. Law and Zhu (2004) introduced a parameter to describe the variation of opening/closing behavior of the crack.

$$\left.\begin{aligned} E(x) &= E_0\left(1 - s(1-\alpha)\cos^2\left(\frac{\pi}{2}\left(\frac{x}{\beta L/2}\right)^n\right)\right), \text{for}(0 < x < \beta L/2) \\ E &= E_0, \text{for}(\beta L/2 \le x \le L/2) \end{aligned}\right\} \tag{9}$$

where s is introduced in open crack model to describe the degradation process, and $0 \le s < 1$. s is equal to 0 or 1 denoting that the crack is closing completely or open completely, respectively; when $0 < s < 1, s = s_0 + (1 - s_0)\sin\left(\frac{\pi v t}{L}\right)$, where $s_0 = 0.3$, v is the speed of the vehicle.

2.3 Time-frequency analysis of the structural acceleration response

2.3.1 A brief introduction to the Hilbert-Huang transform

It is known that the HHT consists of two parts: empirical mode decomposition (EMD) and hilbert spectral analysis (HSA). The HHT is suitable for the nonlinear and non-stationary data analysis (Huang *et al*. 1998). A brief introduction of the method is given below.

Firstly, making use of EMD, the response signal is decomposed into a set of narrow-band signals called the intrinsic mode functions (IMFs). The basis of the EMD method is the "sifting method". Through the sifting process, the original signal is finally expressed as a sum of the IMFs and a residual signal.

$$x(t) = \sum_{j=1}^{n} c_j(t) + r_n(t) \tag{10}$$

where $\sum_{j=1}^{n} c_j(t)$ is the summation of the IMFs, and $r_n(t)$ is the residual signal.

Secondly, the instantaneous frequency is computed through the Hilbert transform on each IMF component. For an IMF $c_j(t)$, whose Hilbert transform is defined as

$$\tilde{c}_j(t) = \frac{1}{\pi}\int \frac{c_j(t)}{t-\tau} d\tau \tag{11}$$

The analytic signal of the j th IMF is

$$z_j(t) = c_j(t) + i\tilde{c}_j(t) = a_j(t)e^{i\theta_j(t)} \tag{12}$$

where i is the imaginary part, $a_j(t) = \sqrt{c_j^2(t) + \tilde{c}_j^2(t)}$, $\tan[\theta_j(t)] = \frac{\tilde{c}_j(t)}{c_j(t)}$. The instantaneous frequency is defined as

$$\omega_j(t) = \frac{d\theta_j(t)}{dt} \tag{13}$$

2.3.2 Wavelet transform

Among the spectrum of time-frequency analysis techniques, the wavelet transform has also received much attention and has been widely used in recent years. The wavelet analysis can provide local features in both time and frequency domains and has the characteristics of multi-scale and "mathematical microscope" (Gurley and Kareem 1999). The continuous wavelet transform of signal $x(t)$ is defined as

$$W(a,t) = \frac{1}{\sqrt{a}}\int_{-\infty}^{\infty} x(\tau)\psi^*\left(\frac{t-\tau}{a}\right) d\tau \tag{14}$$

where $\psi(t)$ is the mother wavelet and $\psi^*(t)$ indicates the complex conjugate of the wavelet function. Parameter t indicates the time shifting. The factor $1/\sqrt{a}$ is used to ensure energy preservation and a is the scale index, which controls the width of the wavelet window. $W(a,t)$ is the transform that decomposes an arbitrary signal $x(t)$ via basis functions with compact support that are simply dilations and translations of the mother wavelet. Therefore, the information can be obtained in both frequency domain and time domain.

The modified Morlet wavelet function is used in this study with the form

$$\psi(t) = \frac{1}{\sqrt{\pi f_b}}(e^{i2\pi f_c t} - e^{-f_b(\pi f_c)^2})e^{-t^2/f_b} \tag{15}$$

where f_b is the bandwidth parameter, f_c is the central wavelet frequency, and i is the imaginary unit.

3. Numerical simulations

3.1 A single-span simply supported bridge

A single-span simply supported bridge subjected to a moving vehicle is studied. The parameters of the bridge are: flexural rigidity $EI = 1.275 \times 10^{11}\ \mathrm{Nm}^2$, mass density $\rho = 2500\ \mathrm{kg/m}^3$ and length $L = 30\ \mathrm{m}$. The parameters of the two-axle vehicle are taken as

$$M_s = 17735\ \mathrm{kg},\ M_{t1} = 1500\ \mathrm{kg},\ M_{t2} = 1000\ \mathrm{kg},\ a_1 = 2.22\ \mathrm{m},\ a_2 = 2.05\ \mathrm{m},$$

$$k_{s1} = 2.47 \times 10^6\ \mathrm{Nm}^{-1},\ k_{s2} = 4.23 \times 10^6\ \mathrm{Nm}^{-1},\ k_{t1} = 3.74 \times 10^6\ \mathrm{Nm}^{-1},\ k_{t2} = 4.60 \times 10^6\ \mathrm{Nm}^{-1},$$

$$c_{s1} = 3 \times 10^4\ \mathrm{Nm}^{-1}s,\ c_{s2} = 4 \times 10^4\ \mathrm{Nm}^{-1}s,\ c_{t1} = 3.90 \times 10^3\ \mathrm{Nm}^{-1}s,\ c_{t2} = 4.30 \times 10^3\ \mathrm{Nm}^{-1s},$$

$$J = 1.47 \times 10^5\ \mathrm{kgm}^2$$

3.1.1 Dynamic response of the bridge

The vehicle is assumed to move from the left end to the right end of the beam with a speed of 10 m/s. The bridge is discretized into 20 Eulerian beam elements. In the calculation of the dynamic response of the bridge-vehicle system, the time step is taken to be 0.005 and the first two modal damping ratios are assumed to be 0.015 and 0.02, respectively. The first four natural frequencies of the intact bridge are 5.69, 22.76, 51.20 and 91.02 Hz, and the natural frequencies of the vehicle are 1.6, 2.3, 10.3 and 15.1 Hz. Fig. 3 shows the vertical deflection time history of the mid-point of bridge. The peak value of the beam is obtained when the rear wheel of the two-axle vehicle reaches the mid-point of the bridge.

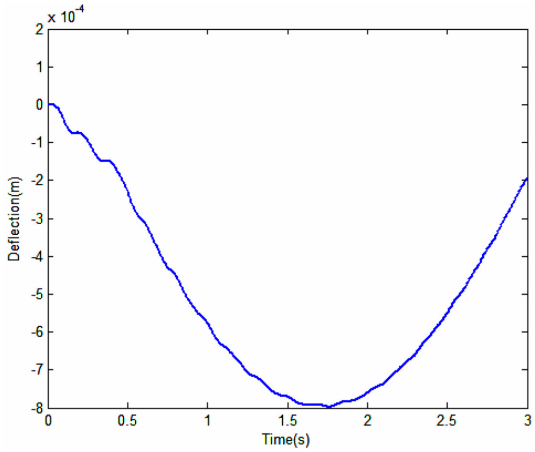

Fig. 3 Dynamic deflection of the intact simply supported bridge

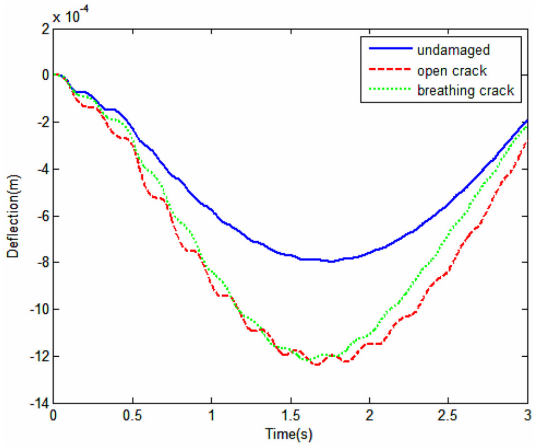

Fig. 4 Dynamic response of the bridge with different crack models

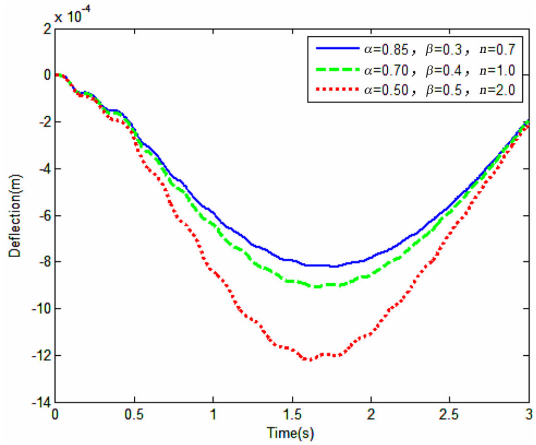

Fig. 5 Dynamic response of the bridge with different crack parameters

The deflection responses of the middle of the bridge with different crack models are showed in Fig. 4. One can observe that there is an obvious increase in the deflection when the crack appears in the beam. This is due to the reduction in the flexural rigidity of the beam when the crack emerges, which affects the load-carrying capacity of the bridge. The maximum values of deflection of the mid-point obtained for the two crack models are almost the same, which indicates that the two models are basically the same when the breathing crack is completely open. As a whole, the deflection obtained from the breathing crack is slightly smaller than that of the open crack, due to the "opening/closing effect" of the breathing crack model.

3.1.2 Dynamic response of the bridge with different crack zones

Since the parameters α, β, n characterize the pattern of crack damage, if they change, the effect of crack on the dynamic responses of the bridge should be different. Let us consider the case when the open crack occurs in the middle of the bridge. Fig. 5 gives a comparison on the deflection

Table 1 First six frequencies of the bridge with different open cracks

Mode number	Intact bridge	$\alpha = 0.9$, $\beta = 0.3$, $n = 0.7$	$\alpha = 0.7$, $\beta = 0.4$, $n = 1$	$\alpha = 0.5$, $\beta = 0.5$, $n = 2$
1	5.68	5.61	5.36	4.63
2	22.75	22.73	22.56	21.26
3	51.20	50.61	49.14	46.23
4	91.02	90.73	88.96	80.89
5	142.23	140.92	138.02	128.71
6	204.82	203.76	199.03	184.68

responses at the mid-span of the bridge with three sets of parameters: $\alpha = 0.85, \beta = 0.3, n = 0.7$, $\alpha = 0.7, \beta = 0.4, n = 1$ and $\alpha = 0.5, \beta = 0.5, n = 2$. Obviously, the crack damage has a negative effect on the responses of the bridge, especially when the crack condition is serious. For the case with $\alpha = 0.5, \beta = 0.5, n = 2$, the maximum deflection is almost doubled compared with that of the intact bridge. Table 1 shows the first six natural frequencies of the bridge with an open crack but different parameters. The natural frequency of the bridge decreases little by little when the crack damage is getting more serious.

3.1.3 Time-frequency analysis of the dynamic response

It is known that the dynamic response of the vehicle-bridge system will reveal nonlinear characteristics due to the existence of breathing crack in the bridge. The "breathing effect" will lead to the change in the natural frequency of the bridge with time, which is known as the instantaneous frequency. In this section, the time-frequency analysis of the acceleration response is carried out using both the HHT and WT.

In recent years, many researchers use the HHT to analyze the non-stationary signals. There are a host of research papers dealing with the improved HHT method. In this paper, the improved HHT (Yang 2008) is adopted. Making use of the HHT, the instantaneous frequency can be obtained. On the other hand, the WT is also studied by many scholars. The Morlet wavelet is used in this study with $f_b = 1, f_c = 3$.

The time-frequency information is extracted using the acceleration response of the bridge with a breathing crack located at the mid-point of the bridge, the parameters of the crack function are taken as: $\alpha = 0.5, \beta = 0.5, n = 2$. Fig. 6 shows the time-frequency curve of the acceleration response at $L/4$ of the bridge. It can be found that the frequency components in the dynamic vibration of the bridge are mainly composed of the first few lower frequencies of the bridge and vehicle. The bridge vibrates mainly at its fundamental frequency of 5.69 Hz. The first and third frequencies of moving vehicle are also contained in the dynamic response of the bridge. Apart from these frequency components, several higher order frequency components (around 30 Hz, 40 Hz) can also be observed from the dynamic response of the bridge. This nonlinear characteristic comes from the effect of the breathing crack in the bridge. Each frequency component and its magnitude of the bridge can be clearly seen in the Hilbert-Huang transform marginal spectrum of the acceleration response shown in Fig. 7.

A comparison study is carried out to analyze the variation of amplitude of each frequency component for different crack parameters. The Hilbert-Huang marginal spectra of accelerations for three different breathing crack conditions are shown in Fig. 8. One can find that the main frequency components of the bridge response are the first three frequencies of the coupled bridge-vehicle

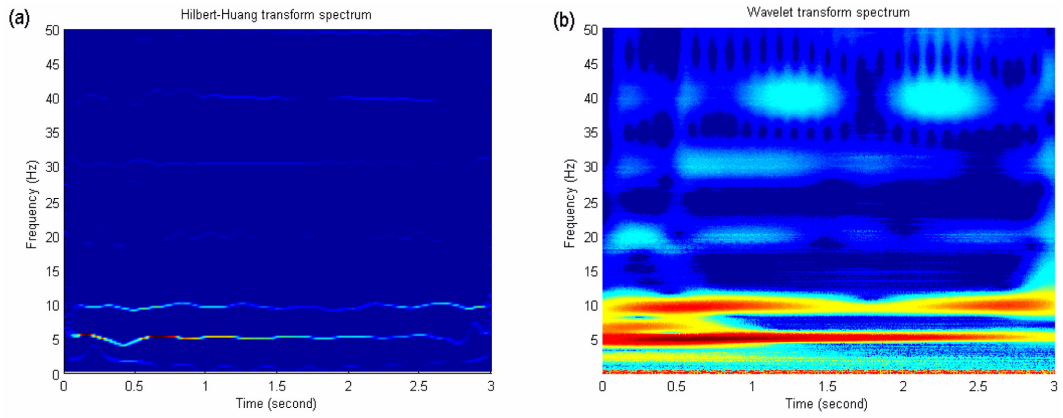

Fig. 6 Time-frequency curve of acceleration of the bridge with a breathing crack: (a) Hilbert-Huang transform spectrum and (b) Wavelet transform spectrum

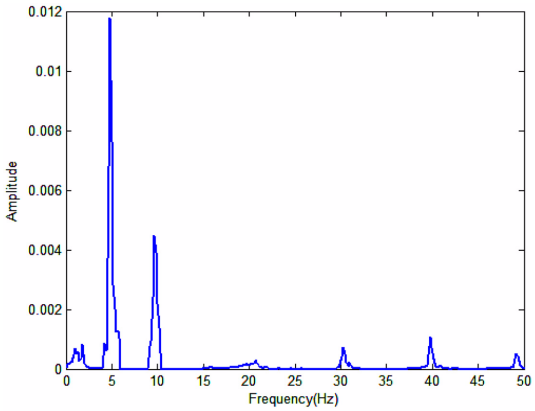

Fig. 7 Hilbert-Huang marginal spectrum of the acceleration response of the bridge with a breathing crack

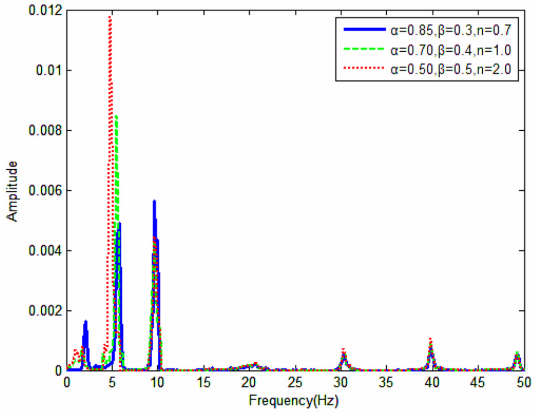

Fig. 8 Hilbert-Huang marginal spectrum of the acceleration response with different crack parameters

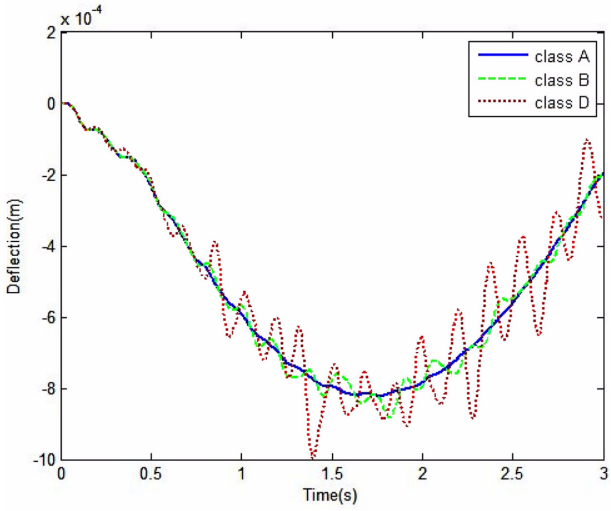

Fig. 9 Dynamic response of the bridge with different road roughness

system. There are also several harmonic components in the frequency components, but their magnitudes are relatively small.

In the case studied above, the road roughness is not considered in the calculation of the dynamic responses. Such an effect will be considered here. The PSD (Law and Zhu 2004) is used to simulate the road surface roughness and classes A, B and D are investigated, with class A indicating the best quality. Fig. 9 shows the deflection of the breathing cracked bridge ($\alpha = 0.85, \beta = 0.3, n = 0.7$) with different levels of road roughness. One can find that the road roughness has significant influence on the dynamic responses of the bridge. The amplitude of the bridge response for class B and class D is much larger than that for class A.

3.2 A three-span continuous bridge

In this example, a three-span continuous bridge is studied, as shown in Fig. 1. The parameters adopted of the bridge are: flexural rigidity $EI = 1.752 \times 10^{11}\ \mathrm{Nm}^2$ mass density $\rho = 2500\ \mathrm{kg/m}^3$, cross-sectional area $A = 7.9725\ \mathrm{m}^2$, $L_1 = 20\ \mathrm{m}, L_2 = 20\ \mathrm{m}, L_3 = 20\ \mathrm{m}$. The parameters of the vehicle are the same as the first example. The first four natural frequencies of the intact bridge are 11.4, 14.6, 21.3 and 45.6 Hz.

Free vibration of the bridge is analyzed to obtain the natural frequencies and the corresponding mode shapes of the bridge with and without crack. The first eight mode shapes of the bridge with and without crack damage are compared in Fig. 10. It is assumed that the crack occurs at the middle point of the mid-span of bridge and the *E*-modulus has a 50% reduction. In this figure, one can find that the differences between the mode shapes of the bridge with and without crack are small.

The first eight natural frequencies of the bridge with and without crack(s) are listed in Table 2. It should be pointed out that the frequency calculated in the table for the case with "breathing" crack is based on the condition of "completely open". From this table, one can find that the natural frequency of the beam decreases due to the presence of cracks.

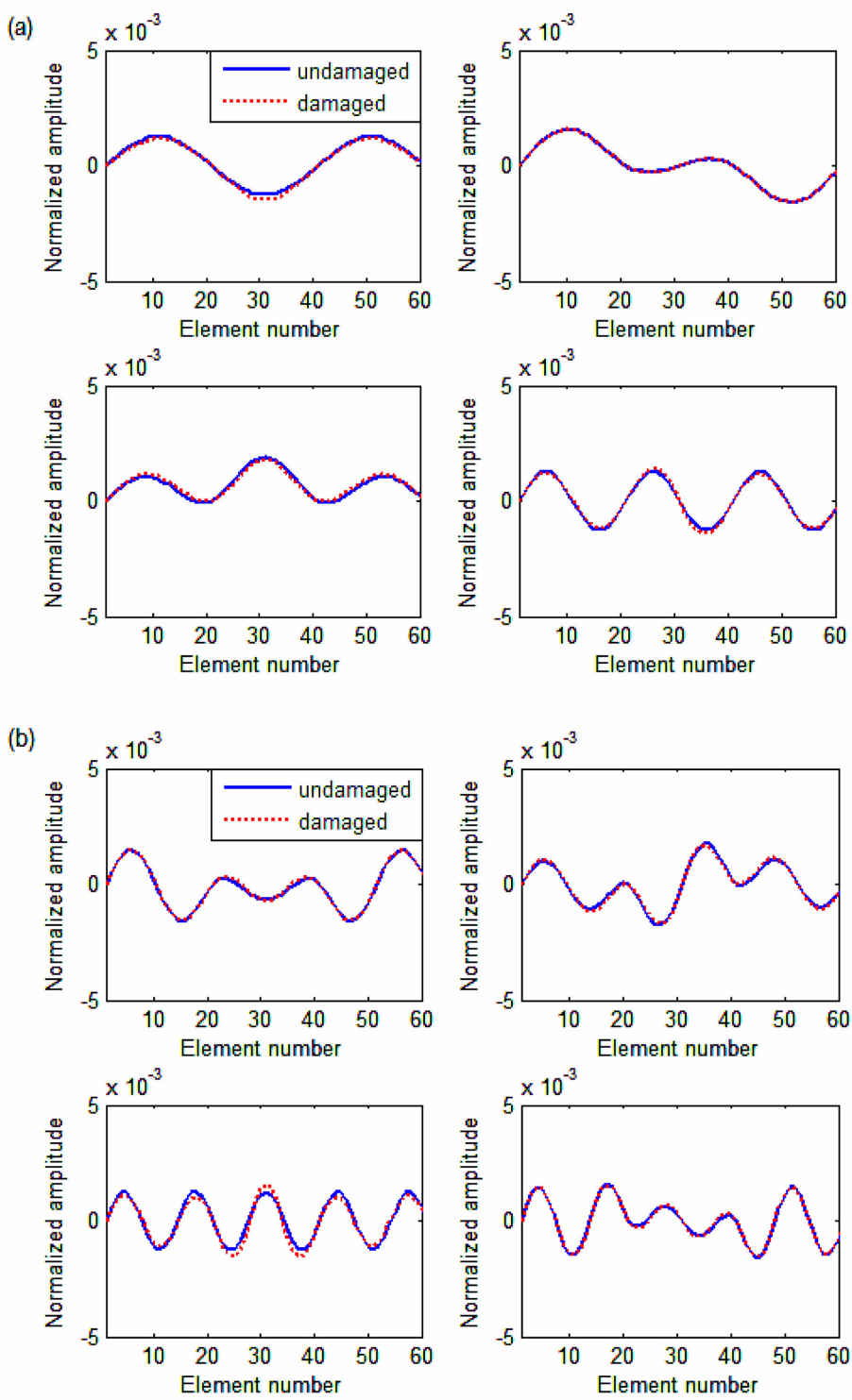

Fig. 10 First eight mode shapes of the three-span bridge: (a) 1st~4th and (b) 5th~8th

Table 2 First eight natural frequencies of the bridge with cracks

Mode number	Intact bridge	A crack at location B	Two cracks at locations A and B	Three cracks at locations A, B and C
1	11.41	10.65	9.88	9.37
2	14.63	14.58	13.71	12.65
3	21.36	20.01	19.59	19.10
4	45.66	44.65	43.68	43.00
5	52.04	51.59	50.14	48.59
6	63.84	61.39	60.41	59.26
7	102.70	98.64	94.91	92.96
8	112.20	111.30	106.80	101.70

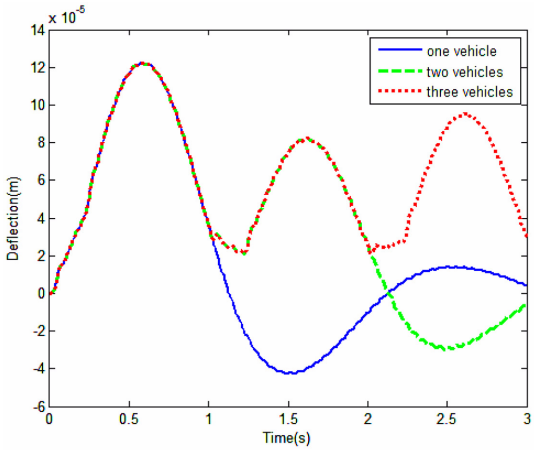

Fig. 11 Displacement response of the left span of bridge with different vehicle numbers

Table 3 Maximum deflections of the mid-point of left-span under different vehicle numbers

Deflections of the bridge (10^{-4} m)	One vehicle	Two vehicles	Three vehicles
Point A	1.223	1.223	1.224

3.2.1 Dynamic response of the intact bridge

In this case, different numbers of vehicles are used to simulate practical traffic flow, three cases are studied: (1) one vehicle, (2) two vehicles and (3) three vehicles. For cases (2) and (3), the vehicles are assumed to move along the bridge from the left support to the right support one by one with a speed of 20 m/s. The distance between each vehicle is 20 m. Fig. 11 shows the deflection time histories of the middle point of the left-span with different numbers of vehicles. Table 3 lists the maximum deflections of the mid-point of the left-span under different vehicle numbers.

3.2.2 Time-frequency analysis of the dynamic response with breathing cracks

For the present purpose, we consider that there are three vehicles moving along the bridge one by one. The parameters of the damage function are taken as: $\alpha = 0.5$, $\beta = 0.5$, $n = 2$. Two cases are studied.

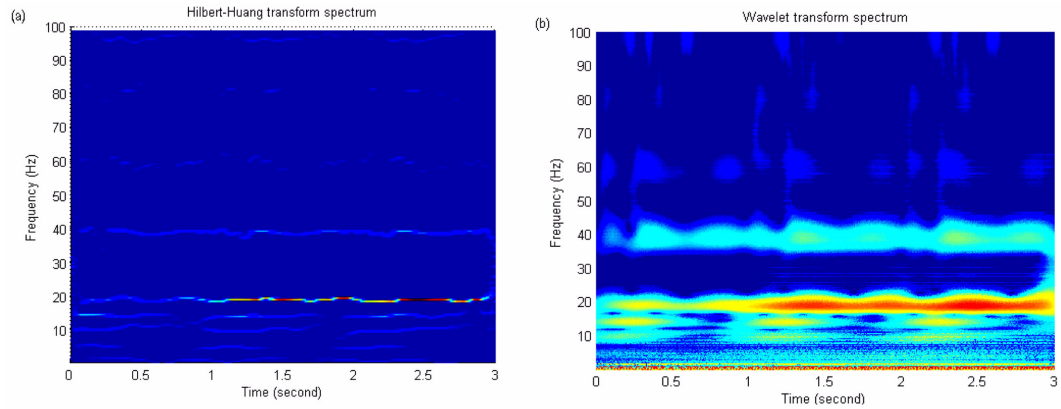

Fig. 12 Time-frequency curve of acceleration of a three-span bridge with one breathing crack: (a) Hilbert-Huang transform spectrum and (b) Wavelet transform spectrum

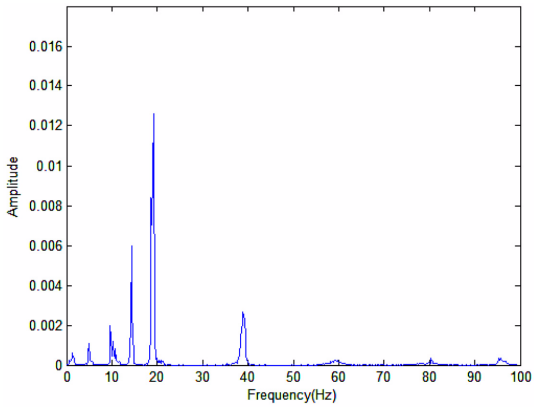

Fig. 13 Hilbert-Huang marginal spectrum of the acceleration response of a three-span bridge with one breathing crack

Case 1: Assuming that only a breathing crack is located at point B as shown in Fig. 1. Figs. 12 and 13 show the time-frequency result from HHT and WT for the acceleration response at a quarter point (from left) of the first span.

Case 2: Assuming that three breathing cracks are located at points A, B and C. Figs. 14 and 15 show the time-frequency result of the acceleration response at a quarter point (from left) of the first span.

The following observations are made for the two cases above:

1. The main frequency components in the time response are the 1st, 2nd and 3rd frequencies of the bridge as shown in Figs. 12 and 14.

2. Due to the nonlinear effect of breathing cracks, there also exist harmonic components in the response. In case 1, the crack is located at the mid-point of the second span, as the vehicle is moving along this span, the depth of the breathing crack changes with the moving loads. From Fig. 12, one can clearly find that the harmonic components near 40, 60 and 100 Hz. Fig. 13 shows the

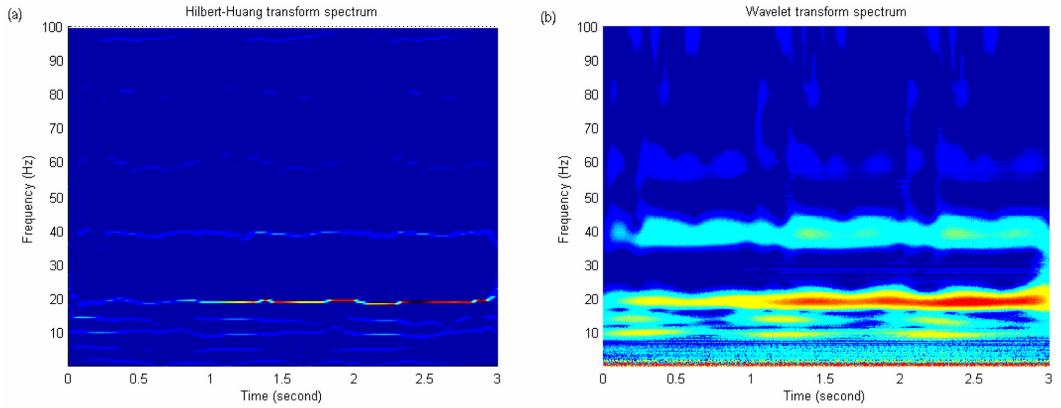

Fig. 14 Time-frequency curve of acceleration of a three-span bridge with three breathing cracks: (a) Hilbert-Huang transform spectrum and (b) Wavelet transform spectrum

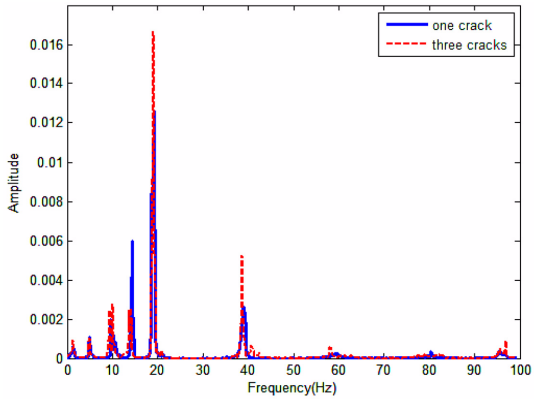

Fig. 15 Hilbert-Huang marginal spectrum with different number of breathing cracks

magnitude of each frequency component. In case 2, we assume that there are three breathing cracks located at points A, B and C, as shown in Fig. 1. From Fig. 14, one can also find that the harmonic components near 40, 60, 80 and 100 Hz.

3. Fig. 15 is the Hilbert-Huang transform marginal spectrum with different breathing crack numbers. Comparing the HHT marginal spectrum of the responses with different crack numbers, the amplitudes of the 3rd and 4th frequency components of the bridge increase if more cracks appear. The harmonic components also become stronger, but their magnitudes are still relatively small.

4. Comparing the time-frequency results from HHT with those from WT, it can be seen that both the HHT and WT can extract the time-frequency characteristics from the bridge responses. The instantaneous frequencies of the system can be identified from the HHT. The wavelet transform can only show the frequency bands and the energy distribution with time, but not the instantaneous frequency.

4. Conclusions

This paper deals with the time-frequency analysis of bridges with open and breathing cracks. The dynamic responses of the vehicle-bridge system are obtained from the Newmark integration method. This study shows that the dynamic responses of the bridge will become large when the crack damage occurs. The time-frequency analysis is conducted for the dynamic responses of the bridge with breathing cracking using both the HHT and wavelet transform. Comparing the time-frequency results from HHT with those from WT, one observes that the time-frequency characteristics can be extracted from both HHT and WT. The frequency bands and the energy distribution can be shown from WT, but the instantaneous frequency can not be identified clearly. The time-frequency results from the HHT indicate that harmonic components will emerge due to the nonlinear effect of the breathing crack(s). The effect of the road roughness on the dynamic responses of the bridge is also investigated. It is concluded that dynamic responses of the bridge will increase when the road roughness becomes serious.

Acknowledgements

This work is supported in part by the NSFC (11172333, 10972241), GDSF (07003680, 9151027501000014), the Guangdong Province Science and Technology Program (2010A030200008, 2011A030200012), Doctoral Program Foundation of Ministry of Education of China (20090171110042), and the Fundamental Research Funds for the Central Universities (09lgpy08). Such financial aids are gratefully acknowledged.

References

Abdel Wahab, M.M., De Roeck, G. and Peeters, B. (1999), "Parameterization of damage in reinforced concrete structures using model updating", *J. Sound Vib.*, **228**(4), 717-730.

An, N., Xia, H. and Zhan, J.W. (2010), "Identification of beam crack using the dynamic response of a moving spring-mass unit", *Interact. Multiscale Mech.*, **3**(4), 321-331.

Ariaei, A., Ziaei-Rad, S. and Ghayour, M. (2009), "Vibration analysis of beams with open and breathing cracks subjected to moving masses", *J. Sound Vib.*, **326**(3-5), 709-724.

Aydin, K. (2008), "Vibratory characteristics of Euler-Bernoulli beams with an arbitrary number of cracks subjected to axial load", *J. Vib. Control.*, **14**(4), 485-510.

Binici, B. (2005), "Vibration of beams with multiple open cracks subjected to axial force", *J. Sound Vib.*, **287**(1-2), 277-295.

Chakraborty, A. and Basu, B. (2008), "Nonstationary response analysis of long span bridges under spatially varying differential support motions using continuous wavelet transform", *J. Eng. Mech.-ASCE*, **134**(2), 155-162.

Chang, K.C., Wu, F.B. and Yang, Y.B. (2010), "Effect of road surface roughness on indirect approach for measuring bridge frequencies from a passing vehicle", *Interact. Multiscale Mech.*, **3**(4), 299-308.

Chen, W.H., Lu, Z.R., Lin, W., Chen, S.H., Ni, Y.Q., Xia, Y. and Liao, W.Y. (2011), "Theoretical and experimental modal analysis of the Guangzhou New TV Tower", *Eng. Struct.*, **33**(12), 3628-3646.

Chondros, T.G., Dimarogonas, A.D. and Yao, J. (2001), "Vibration of a beam with a breathing crack", *J. Sound Vib.*, **239**(1), 57-67.

Cojocaru, E.C. and Irschik, H. (2010), "Dynamic response of an elastic bridge loaded by a moving elastic beam with a finite length", *Interact. Multiscale Mech.*, **3**(4), 343-363.

Douka, E. and Hadjileontiadis, L.J. (2005), "Time-frequency analysis of the free vibration response of a beam with a breathing crack", *NDT&E Int.*, **38**(1), 3-10.
Gurley, K. and Kareem, A. (1999), "Applications of wavelet transforms in earthquake, wind and ocean engineering", *Eng. Struct.*, **21**(2), 149-167.
Huang, N.E., Shen, Z., Long, S.R., Wu, M.C., Shih, H.H., Zheng, Q., Yen, N.C., Tung, C.C. and Liu, H.H. (1998), "The empirical mode decomposition and the Hilbert spectrum for non-linear and non-stationary time series analysis", *Proceedings of the Royal Society of London Series A-Mathematical Physical and Engineering Sciences*, **454**, 903-995.
Kim, H. and Melhem, H. (2003), "Fourier and wavelet analyses for fatigue assessment of concrete beams", *Exp. Mech.*, **43**(2), 131-140.
Kou, J.W. and Dewolf, J.T. (1997), "Vibrational behavior of continuous span highway bridge-influencing variables", *J. Struct. Eng.-ASCE*, **123**(3), 333-344.
Law, S.S. and Zhu, X.Q. (2004), "Dynamic behavior of damaged concrete bridge structures under moving vehicular loads", *Eng. Struct.*, **26**(9), 1279-1293.
Law, S.S. and Zhu, X.Q. (2005), "Nonlinear characteristics of damaged concrete structures under vehicular load", *J. Struct. Eng.-ASCE*, **131**(8), 1277-1285.
Li, Q.S. and Wu, J.R. (2007), "Time-frequency analysis of typhoon effects on a 79-storey tall building", *J. Wind Eng. Ind. Aerod.*, **95**(12), 1648-1666.
Li, X.Z. and Zhu, Y. (2010), "Stochastic space vibration analysis of a train-bridge coupling system", *Interact. Multiscale Mech.*, **3**(4), 333-342.
Lu, Z.R. and Law, S.S. (2009), "Dynamic condition assessment of a cracked beam with the composite element model", *Mech. Syst. Signal Pr.*, **23**(2), 415-431.
Mahmoud, M.A. and Abou Zaid, M.A. (2002), "Dynamic response of a beam with a crack subject to a moving mass", *J. Sound Vib.*, **256**(4), 591-603.
Mahmoud, M.A. (2001), "Stress intensity factors for single and double edge cracks in a simple beam subject to a moving load", *Int. J. Fracture*, **111**(2), 151-161.
Pan, T.C. and Li, J. (2002), "Dynamic vehicle element method for transient response of coupled vehicle-structure systems", *J. Struct. Eng.-ASCE*, **128**(2), 214-223.
Sun, L. and Luo, F. (2007), "Non-stationary dynamic pavement loads generated by vehicles traveling at varying speed", *J. Transp. Eng.*, **133**(4), 252-263.
Wang, S.Q., Xia, H., Guo, W.W. and Zhang, N. (2010), "Nonlinear dynamic response analysis of a long-span suspension bridge under running train and turbulent wind", *Interact. Multiscale Mech.*, **3**(4), 309-320.
Yang, J.R., Li, J.Z. and Chen, Y.H. (2010), "Vibration analysis of CFST tied-arch bridge due to moving vehicles", *Interact. Multiscale Mech.*, **3**(4), 389-403.
Yang, W.X. (2008), "Interpretation of mechanical signals using an improved Hilbert-Huang transform", *Mech. Syst. Signal Pr.*, **22**(5), 1061-1071.
Yang, Y.B. and Yau, J.D. (1997), "Vehicle-bridge interaction element for dynamic analysis", *J. Struct. Eng.-ASCE*, **123**(11), 1512-1518.
Yau, J.D. (2009), "Vehicle/bridge interactions of a rail suspension bridge considering support movements", *Interact. Multiscale Mech.*, **2**(3), 263-276.
Yener, M. and Chompooming, K. (1994), "Numerical method of lines for analysis of vehicle-bridge dynamic interaction", *Comput. Struct.*, **53**(3), 709-726.
Zhang, R.R., King, R., Olson, L. and Xu, Y.L. (2005), "Dynamic response of the Trinity River Relief Bridge to controlled pile damage: modeling and experimental data analysis comparing Fourier and Hilbert-Huang techniques", *J. Sound Vib.*, **285**(4-5), 1049-1070.
Zhu, X.Q. and Law, S.S. (2007), "Nonlinear characteristics of damaged reinforced concrete beam from Hilbert-Huang Transform", *J. Struct. Eng.-ASCE*, **133**(8), 1186-1191.